

A Single Phase Multilevel Current-Source Inverter For Distributed Generation

Naresh Masiboina, naresh.masiboina@gmail.com

Abstract—In this paper, a multilevel current-source inverter (MCSI) topology is utilized with distributed energy sources. The single-rating inductor MCSI is explored, taking advantage of the features of field-programmable gate arrays (FPGA) for control and gate signal generation. The proposed topology is built with identical modules where all inductors carry the same amount of current, simplifying the construction and operation of industrial applications with higher efficiency. A new state-machine approach, which is easy to implement in an FPGA, and a proper implementation of the phase-shifted carrier sinusoidal pulse width modulation (PSC-SPWM) allow both current balance in all modules and effective switching-frequency minimization. The studied performance of the MCSI topology in the distributed generation proposed offers strong advantages such as improved output waveforms. Simulation and experimental results show the effectiveness of the proposed solution.

Index Terms—Field-programmable gate array (FPGA), multilevel current-source inverter (MCSI), phase-shifted carrier SPWM (PSC-SPWM), distributed generation.

I. INTRODUCTION

With increasing concern of global warming and the depletion of fossil fuel reserves, many are looking at sustainable energy solutions to preserve the earth for the future generations. Other than hydro power, photovoltaic energy holds the most potential to meet our energy demands. Alone, solar energy is capable of supplying large amounts of power but its presence is highly unpredictable as it can be here one moment and gone in another. Similarly, solar energy is present throughout the day but the solar irradiation levels vary due to sun intensity and unpredictable shadows cast by clouds, birds, trees, etc. Fuel Cell converts the chemical energy to electrical energy with higher efficiency.

The common inherent drawback of photovoltaic systems is their intermittent natures that make them unreliable. However, by combining these two intermittent sources and by incorporating maximum power point tracking (MPPT) algorithms, the system's power transfer efficiency and reliability can be improved significantly. The integration of renewable energy sources and energy-storage systems has been one of the new trends in power-electronic technology. The increasing number of renewable energy sources and distributed generators requires new strategies for their operations in order to maintain or improve the power-supply stability and quality. Combining multiple renewable resources via a common dc bus of a power converter has been prevalent because of convenience in integrated monitoring and control and consistency in the structure of controllers as compared with a common ac type. Dynamic performance of Fuel cell and solar system is analyzed. A system model was developed and compared with a real system. Several methodologies for optimal design or unit sizing.

Most applications are for stand-alone operation, where the main control target is to balance local loads. A

few grid-connected systems consider the grid as just a back-up means to use when there is insufficient supply from renewable sources. They are originally designed to meet local load demands with a loss of power-supply probability of a specific period. Such hybrid systems, focusing on providing sustainable power to their loads, do not care much about the quality or flexibility of power delivered to the grid. From the perspective of utility, however, a hybrid system with less fluctuating power injection or with the capability of flexibly regulating its power is more desirable. In addition, users will prefer a system that can provide multiple options for power transfer since it will be favorable in system operation and management. Control strategies of such a hybrid system should be quite different from those of conventional systems.

Classical techniques of maximum power tracking are applied in PV array control. Dynamic modeling and simulations were based on Power System Computer Aided Design with MATLAB/SIMULINK. The program was based on Dommel's algorithm, specifically developed for the simulation of high-voltage direct current systems and efficient for the transient simulation of power system under power-electronic control.

In this paper, a single-rating inductor MCSI is employed to feed a three-phase load. The converter consists of a number of identical modules, which determine the different current levels. Each module uses two balance inductors and six power switches. All inductors of every module should carry the same amount of current. The current flowing through the inductors can be balanced, and switching frequency can be reduced by applying a state-machine modulation that properly uses redundant zero states. Industrial assemblies are easy to develop and to operate because all modules are identical. The behavior of this converter is very different from the behavior of the traditional MVSI. Herein, each module carries a fraction of the load current, and there is no separation of modules or switches per phase as occur in an MVSI. In most MVSI, when a low voltage is delivered to the load, the outermost switches stop working, and the load current is only delivered by the switches connected close to the central point of the converter. This situation does not occur with the topology used for this MCSI. This converter with the proposed modulation always splits the output current among all the switches regardless of the modulation index (ma).

The modulation and gate-drive control logic are implemented on a field-programmable gate array (FPGA), which is a power-ful cost-effective solution. It allows complex logical and control algorithms, fast speed, and multiple input/output pins, which becomes particularly attractive for multilevel-converter control.

The behavior of the MCSI and the modulation technique has been previously presented. In this paper, the SPWM logic

has been modified for better performance and FPGA implementation. A simple approach is presented showing that current balance can be provided by adapting a well-known SPWM strategy while minimizing switching speed using a novel sequential machine design. Finally, a prototype is built to obtain experimental results that validate the proposal

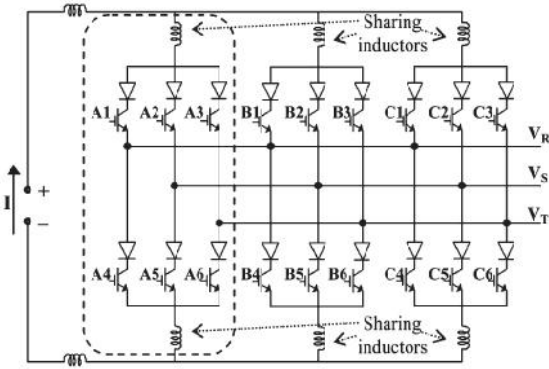


Fig.1. Basic MCSI scheme

CSI ARRANGEMENT:

Switching Structure

The converter topology shown in Fig. 1 consists of multiple CSI subcircuits, sharing a common current source and connected in parallel with the load. Each group of six switches and two inductors will be referred as a module. In this inverter, also known as the “single-rating inductor MCSI,” the sharing inductors split in equal shares the current from the main source. The inductors in series with the main source require a careful design of the startup process of the main current source. The modular structure is the main advantage of this MCSI configuration, where each identical module handles only a fraction of the load current decreasing the overall switching losses [12]. The number of levels n in the output current can

be determined according to the number of modules m in $n = 2m + 1$. (1)

In this paper, we consider $m = 3$ to obtain a load current with seven levels: $I, 2/3I, 1/3I, 0, -1/3I, -2/3I,$ and $-I$. The seven levels in the output current can be achieved by 18 switches with bidirectional voltage blocking capability. Depending on the power and frequency required by the application, the switches could be implemented by MOS transistors, IGBT, ETO, or IGCT, among others, with the addition of series diodes. By turning on and off each switch, different load currents can be obtained. An example of a valid switch combination is shown in Fig. 2, and its corresponding switches states are presented in Table I. Since each branch conducts a third of the supply current I and switches A1, B1, and C1 are on, then current into phase R equals I . The current in phase S is $I/3$ flowing from the load to the source through switch A5, and the current in

phase T is $2/3I$ flowing toward the source through switches B6 and C6. It is worth noting that each output current level can be generated by more than one combination of switches. This redundancy gives more degrees of freedom than the MVSI to minimize the switching frequency of the converter and to balance the current of all the inductors.

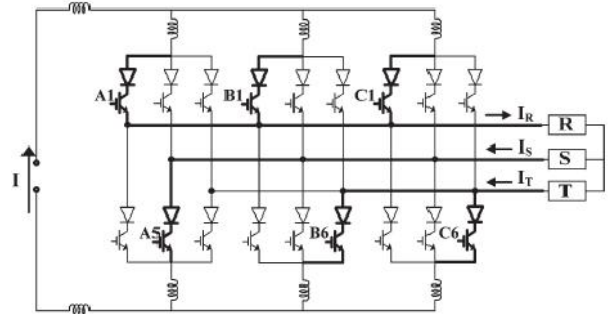


Fig.2. Current flow for a given switch configuration

TABLE I
SWITCHING COMBINATIONS FOR EXAMPLES IN FIG. 2

Sw	A1	A2	A3	A4	A5	A6	B1	B2	B3	B4	B5	B6	C1	C2	C3	C4	C5	C6
State	1	0	0	0	1	0	1	0	0	0	0	1	1	0	0	0	0	1

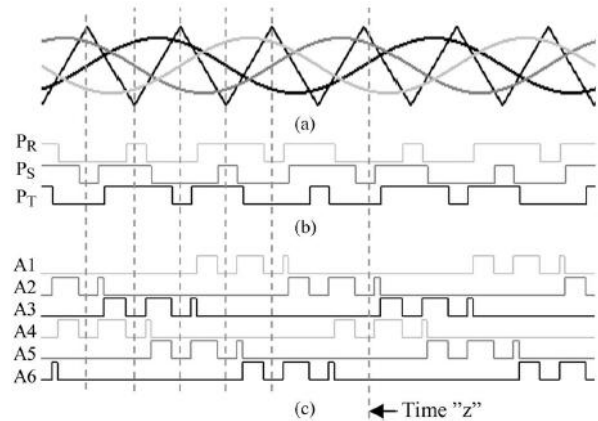


Fig.3. SPWM modulation

SPWM is based on the comparison of a sinusoidal control signal with a triangular carrier. The switches on a single branch are turned on or off depending on whether the control signal is greater or smaller than the carrier.

In SPWM for VSIs, the signals $PR, PS,$ and PT [see Fig. 3(b)] are generated by the comparison of one triangular with three sine waves [see Fig. 3(a)], and they directly drive the switches of each leg of the VSI. To generate the desired current level at the load while assuring current continuity in all the inductors, the driving signals for a CSI [see Fig. 3(c)] need more logic manipulation [28]. The signals Pi are logically subtracted (unsigned) two at a time to generate the firing signal of each switch (A1–A6), according to the logic diagram shown in Fig. 4.

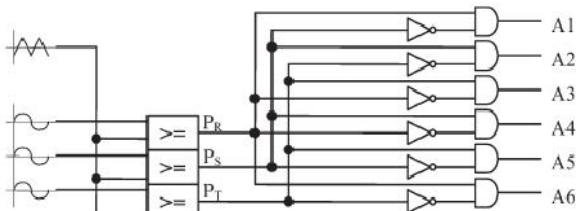


Fig.4. Gate-signal logic diagram

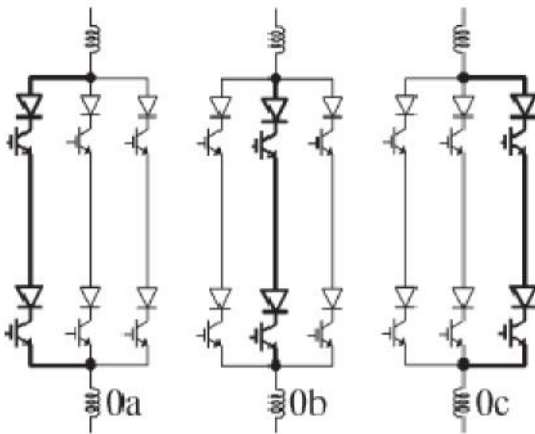


Fig.5. Three different zero states

Multilevel Operation:

To achieve multilevel output current in the load, multiple modules are arranged. Seeking for a current balance over the sharing inductors, a phase-shifted carrier (PSC) SPWM was adopted [27], [31]. The number of modules of the converter will turn into the quantity of triangular carriers that are delayed an angle of

$$k=2 \cdot k/m \quad k=1, 2, \dots, m \quad (2)$$

where m is the number of modules. In a similar way to MVSIs, the effective switching frequency of the current at the load will be $m \cdot f$, where f is the commutation frequency of each module [32]. This allows faster dynamic response and easy filtering of the switching components. The output waveform and spectrum of the proposed MCSI are compared with a three-level CSI in Fig. 6, where all the power device switch at the same frequency and the multilevel topology shift the current spectrum to higher frequencies. The complete modulation block diagram for the three module seven-level converter is shown in Fig. 7

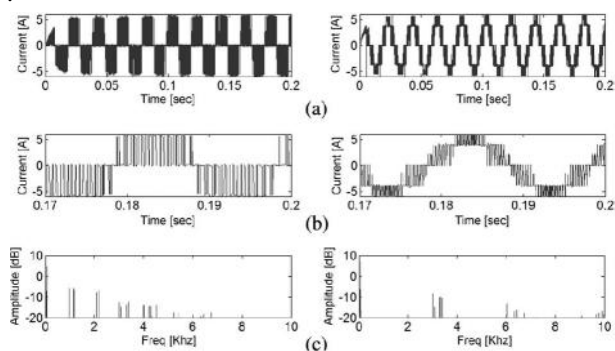


Fig.6. Comparison of three-level CSI and the seven-level MCSI. (a) Output current waveform. (b) Output current waveform detail. (c) Output current spectra.

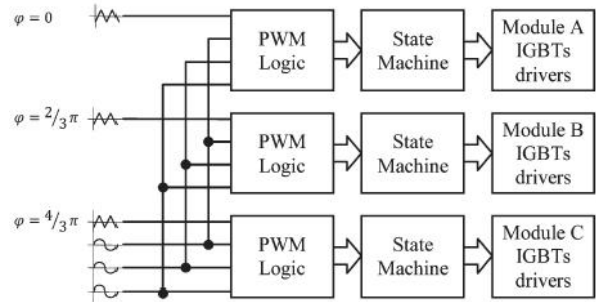


Fig.7. Modulation diagram for the seven-level inverter

Simulation results:

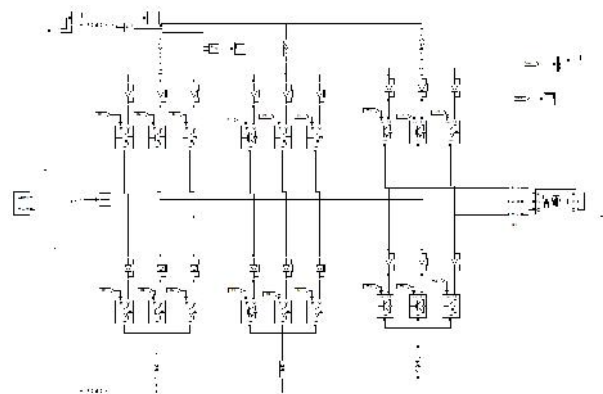


Fig. 8 Matlab Simulation circuit

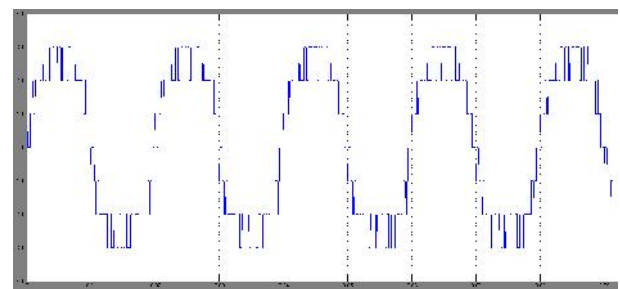


Fig. 9 seven level output

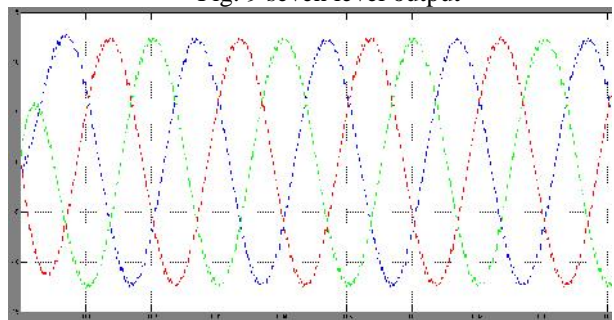


Fig 10 Load Current

The performance of the proposed converter is simulated with Mat lab Simulink. The converter arrangement is composed of three identical modules, each one built with six IGBTs with series diodes. The models used in the simulation match the characteristics of the transistors used in the prototype at an adequate level to give confidence on the validity of the simulation. Moreover, the results have been validated with a detailed PSPICE simulation. The sequential state machine for each module is implemented with Simulink state flow tool. The output current of the simulated inverter is shown in

Fig. 11(a), where the seven levels (I , $2/3I$, $1/3I$, 0 , $-1/3I$, $-2/3I$, $-I$) can be recognized. The output current is filtered by the small capacitor bank delivering a sinusoidal current to the load [see Fig. 11(b)]. Fig. 12 shows the balanced operation of all sharing inductors. It is clear that each inductor carries an average value of one third of the main current even during the startup. A detail of one of these currents is shown in Fig. 12(b).

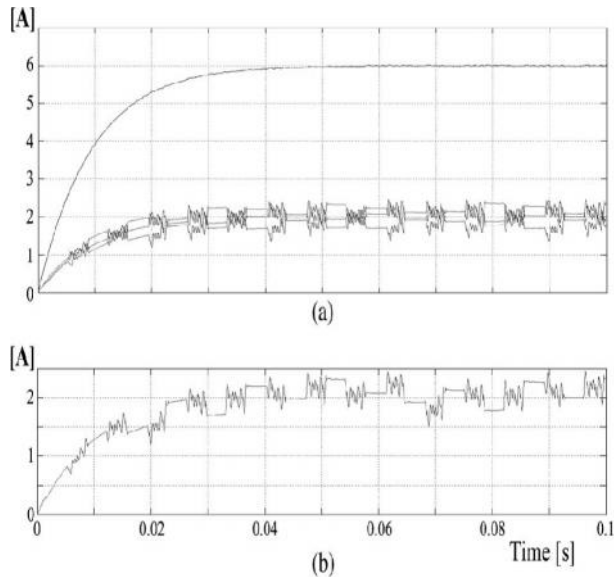


Fig. 12. Inductor current balance. (a) Inductor current. (b) Sharing inductor current detail.

IV. CONCLUSION

The behavior of a seven-level three-module arrangement with distributed energy source was simulated, showing outstanding conditions of load regulation, linearity, and dynamic response. The topology adopted allows operation with high efficiency by reducing the current through the inductors and the losses in the switches. The dynamic response of the output current is satisfactory, both the steady-state and transient behaviors show no voltage spikes or current unbalances, and low-frequency current harmonics are reduced according to the structure

implemented and the advanced switching method used; thus fully functional.

REFERENCES

- [1] R. C. Dugan and T. E. McDermott, "Distributed generation," *IEEE Ind. Appl. Mag.*, vol. 8, no. 2, pp. 19–25, Mar./Apr. 2002.
- [2] R. H. Lasseter, "Microgrids and distributed generation," *J. Energy Eng.*, vol. 133, no. 3, pp. 144–149, Sep. 2007.
- [3] C. Mozina, "Impact of green power distributed generation," *IEEE Ind. Appl. Mag.*, vol. 16, no. 4, pp. 55–62, Jul./Aug. 2010.
- [4] *IEEE Recommended Practice for Utility Interface of Photovoltaic(PV) Systems*, IEEE Standard 929-2000, 2000.
- [5] *IEEE Standard for Interconnecting Distributed Resources with Electric Power Systems*, IEEE Standard 1547-2003, 2003.
- [6] J. Stevens, R. Bonn, J. Ginn, and S. Gonzalez, *Development and Testing of an Approach to Anti-Islanding in Utility-Interconnected Photovoltaic Systems*. Livermore, CA, USA: Sandia National Laboratories, 2000.
- [7] A. M. Massoud, K. H. Ahmed, S. J. Finney, and B. W. Williams, "Harmonic distortion-based island detection technique for inverter-based distributed generation," *IET Renewable Power Gener.*, vol. 3, no. 4, pp. 493–507, Dec. 2009.
- [8] T. Thacker, R. Burgos, F. Wang, and D. Boroyevich, "Single-phase islanding detection based on phase-locked loop stability," in *Proc. 1st IEEE Energy Convers. Congr. Expo.*, San Jose, CA, USA, 2009, pp. 3371–3377.
- [9] S.-K. Kim, J.-H. Jeon, J.-B. Ahn, B. Lee, and S.-H. Kwon, "Frequencyshift acceleration control for anti-islanding of a distributed-generation inverter," *IEEE Trans. Ind. Electron.*, vol. 57, no. 2, pp. 494–504, Feb. 2010.
- [10] A. Yafaoui, B. Wu, and S. Kouro, "Improved active frequency drift antiislanding detection method for grid connected photovoltaic systems," *IEEE Trans. Power Electron.*, vol. 27, no. 5, pp. 2367–2375, May 2012.
- [11] J. M. Guerrero, L. Hang, and J. Uceda, "Control of distributed uninterruptible power supply systems," *IEEE Trans. Ind. Electron.*, vol. 55, no. 8, pp. 2845–2859, Aug. 2008.
- [12] M. C. Chandorkar, D. M. Divan, and R. Adapa, "Control of parallel connected inverters in standalone AC supply systems," *IEEE Trans. Ind. Appl.*, vol. 29, no. 1, pp. 136–143, Jan./Feb. 1993.
- [13] Y. Li, D. M. Vilathgamuwa, and P. C. Loh, "Design, analysis, and realtime testing of a controller for multibus microgrid system," *IEEE Trans. Power Electron.*, vol. 19, no. 5, pp. 1195–1204, Sep. 2004.
- [14] F. Gao and M. R. Iravani, "A control strategy for a distributed generation unit in grid-connected and autonomous modes of operation," *IEEE Trans. Power Del.*, vol. 23, no. 2, pp. 850–859, Apr. 2008.
- [15] S.-H. Hu, C.-Y. Kuo, T.-L. Lee, and J. M. Guerrero, "Droop-controlled inverters with seamless transition between islanding and grid-connected operations," in *Proc. 3rd IEEE Energy Convers. Congr. Expo.*, Phoenix, AZ, USA, 2011, pp. 2196–2201.
- [16] L. Arnedo, S. Dwari, V. Blasko, and S. Park, "80 kW hybrid solar inverter for standalone and grid connected applications," in *Proc. 27th IEEE Appl. Power Electron. Conf. Expo.*, Orlando, FL, USA, 2012, pp. 270–276.
- [17] R. Tirumala, N. Mohan, and C. Henze, "Seamless transfer of gridconnected PWM inverters between utility-interactive and stand-alone modes," in *Proc. 17th IEEE Appl. Power*

- Electron. Conf. Expo.*, Dallas, TX, USA, 2002, pp. 1081–1086.
- [18] R. Teodorescu and F. Blaabjerg, “Flexible control of small wind turbines with grid failure detection operating in stand-alone and grid-connected mode,” *IEEE Trans. Power Electron.*, vol. 19, no. 5, pp. 1323–1332, Sep. 2004.
- [19] H. Zeineldin, M. I. Marei, E. F. El-Saadany, and M. M. A. Salama, “Safe controlled islanding of inverter based distributed generation,” in *Proc. 35th IEEE Power Electron. Spec. Conf.*, Aachen, Germany, 2004, pp. 2515–2520.
- [20] H. Zeineldin, E. F. El-Saadany, and M. M. A. Salama, “Intentional islanding of distributed generation,” in *Proc. IEEE Power Eng. Soc. Gen.Meeting*, San Francisco, CA, USA, 2005, pp. 1496–1502.
- [21] S. Jung, Y. Bae, S. Choi, and H. Kim, “A lowcost utility interactive inverter for residential fuel cell generation,” *IEEE Trans. Power Electron.*, vol. 22, no. 6, pp. 2293–2298, Nov. 2007.
- [22] R. Majumder, A. Ghosh, G. Ledwich, and F. Zare, “Control of parallel converters for load sharing with seamless transfer between grid connected and islanded modes,” in *Proc. IEEE Power Eng. Soc. Gen. Meeting*, Pittsburgh PA, USA, 2008, pp. 1–7.
- [23] H. Tao, J. L. Duarte, and M. A. M. Hendrix, “Line-interactive UPS using a fuel cell as the primary source,” *IEEE Trans. Ind. Electron.*, vol. 55, no. 8, pp. 3012–3021, Aug. 2008.
- [24] D. N. Gaonkar, G. N. Pillai, and R. N. Patel, “Seamless transfer of microturbine generation system operation between grid-connected and islanding modes,” *Electr. Power Compon. Syst.*, vol. 37, no. 2, pp. 174–188, Jan. 2009.
- [25] N. Reza, G. Gevorg, A. Mehrdad, and M. Mishel, “Grid-tied and standalone operation of distributed generation modules aggregated by cascaded boost converters,” *J. Power Electron.*, vol. 10, no. 1, pp. 97–105, Jan. 2010.